

Novel compact and lightweight coaxial C-band transit-time oscillator

Xiao-Bo Deng(邓晓波), Jun-Tao He(贺军涛), Jun-Pu Ling(令钧溥), Bing-Fang Deng(邓秉方), Li-Li Song(宋莉莉), Fu-Xiang Yang(阳福香), Wei-Li Xu(徐伟力)

Citation: Chin. Phys. B . 2020, 29(9): 095205 . **doi:** 10.1088/1674-1056/ab9618
Journal homepage: http://cpb.iphy.ac.cn; http://iopscience.iop.org/cpb

What follows is a list of articles you may be interested in

Novel transit-time oscillator (TTO) combining advantages of radial-line and axial TTO

Wei-Li Xu(徐伟力), Jun-Tao He(贺军涛), Jun-Pu Ling(令钧溥), Li-Li Song(宋莉莉), Bing-Fang Deng(邓秉方), Ouzhixiong Dai(戴欧志雄), Xing-Jun Ge(葛行军)

Chin. Phys. B . 2019, 28(8): 085201 . **doi:** 10.1088/1674-1056/28/8/085201

Nonlinear ion-acoustic solitary waves in an electron-positron-ion plasma with relativistic positron beam

Ridip Sarma, Amar P Misra, Nirab C Adhikary

Chin. Phys. B . 2018, 27(10): 105207 . **doi:** 10.1088/1674-1056/27/10/105207

Schamel equation in an inhomogeneous magnetized sheared flow plasma with *q*-nonextensive trapped electrons

Shaukat Ali Shan, Qamar-ul-Haque

Chin. Phys. B . 2018, 27(2): 025203 . **doi:** 10.1088/1674-1056/27/2/025203

Kadomtsev–Petviashvili equation for dust ion-acoustic solitons in pair-ion plasmas

Hafeez Ur-Rehman

Chin. Phys. B . 2013, 22(3): 035202 . **doi:** 10.1088/1674-1056/22/3/035202

Novel compact and lightweight coaxial C-band transit-time oscillator*

Xiao-Bo Deng(邓晓波), Jun-Tao He(贺军涛)†, Jun-Pu Ling(令钧溥), Bing-Fang Deng(邓秉方), Li-Li Song(宋莉莉), Fu-Xiang Yang(阳福香), and Wei-Li Xu(徐伟力)

College of Advanced Interdisciplinary Studies, National University of Defense Technology, Changsha 410073, *China*

(Received 28 March 2020; revised manuscript received 8 May 2020; accepted manuscript online 25 May 2020)

Compactness and miniaturization have become increasingly important in the development of high-power microwave devices. Based on this rising demand, a novel C-band coaxial transit-time oscillator (TTO) with a low external guiding magnetic field is proposed and analyzed. The proposed device has the following advantages: simple structure, short axial length, high power conversion efficiency, and low external guiding magnetic field, which are of great significance for developing the compact and miniaturized high-power microwave devices. The application of a shorter axial length is made possible by the use of a transit radiation mechanism. Also, loading the opening foil symmetrically to both ends of the buncher helps reduce the external magnetic field of the proposed device. Unlike traditional foils, the proposed opening foil has a circular-hole; therefore, the electron beam will not bombard the conductive foil to generate plasma. This makes it possible to realize long pulse and high repetition rate operation of the device in future experiments. Through numerical calculation and PIC particle simulation, the stability of the intense relativistic electron beam (IREB) and the saturation time of the device are improved by using the conductive foil. The voltage and current of the diode are 548 kV and 11.4 kA, respectively. Under a 0.4-T external guiding magnetic field, a C-band output microwave with a frequency of 4.27 GHz and power of 1.88 GW can be generated. The power conversion efficiency of the proposed device is about 30%.

Keywords: low guiding magnetic field, foil focus, simple structure, short axial length

PACS: 52.35.Fp **DOI:** 10.1088/1674-1056/ab9618

1. Introduction

In recent years, there have been huge strides in the development of high-power microwave technology, and as more and more applications require high power microwave (HPM) generation devices, their development has been leaning towards miniaturization and compactness. Traditional HPM generation devices often have a large guiding magnetic field, which makes the corresponding excitation system to be bulky. Therefore, reducing the strength of the external guiding magnetic field has now become an important development direction for the improvement of device compactness and realization of device miniaturization.

In order to improve the compactness and miniaturization of HPM generation devices, some researchers have tried to remove the external guiding magnetic field. According to previous reports, the Russian Institute of High Current Electronics (IHCE) has carried out simulation and experimental studies on high power Cerenkov devices without guiding magnetic field,[1–4] but the effect of beam–wave interaction is very low because of the lack of guiding magnetic field. This limits the improvement of the power conversion efficiency of such devices, whose experimental efficiency is only 10%–20%. Moreover, the plasma generated when the diffuse electron beam bombards the structure surface of the device may lead to a phenomenon of pulse-shortening thereby affecting the stability of the device. There are other HPM generators without guiding magnetic field, such as mangnetically insulated transmission line oscillator (MILO),[5–7] but the power conversion efficiency of such a device is still very low.

Based on the above researches, the application prospect of HPM generation devices without external guiding magnetic field does not show much promise due to their low power conversion efficiency. So, it is worthwhile to explore miniaturized and compact devices with low external guiding magnetic field but which have high operational stability and high power conversion efficiency. Due to its structural characteristics, the transit time oscillator does not have particularly high requirements for the external guiding magnetic field. Thus, it has great potential for generating high power conversion efficiency and realizing the compactness and miniaturization of the device.

There has been considerable research on transit time oscillators and many valuable findings have been obtained. In Refs. [8,9] conducted were simulation and experiment on a low-magnetic coaxial transit-time oscillator, and the results showed that the experimental efficiency and simulation efficiency were almost the same, but the experimental efficiency

*Project supported by the National Natural Science Foundation of China (Grant No. 61701516).

†Corresponding author. E-mail: hejuntao12@163.com

© 2020 Chinese Physical Society and IOP Publishing Ltd

was only about 20%. By introducing conducting foils, the device can operate without any external guiding magnetic field,[10] however, the IREB bombard conductive foil can easily generate plasma, which is not conducive to long pulse repetitive operation. For this reason, how to enhance both the power conversion efficiency and stability of the device, and further reduce the value of the external guiding magnetic field has become an urgent problem to be solved.

In this paper, the opening foils are loaded in the transmission system, and when the electron beam passes through the opening foils, mirror-image charges are generated on the foils. These charges then exert a radial force on the electron beam, thereby improving the stability of the IREB This means that the beam wave interaction is more complete and the power conversion efficiency is much higher. Because the opening foils improve the quality factor of the device, the saturation time of the device is also shortened. Additionally, the pulse-shortening phenomenon has also been resolved because the electron beam will no longer bombard the opening foils.

The rest of this paper is organized as follows. Section 2 gives a detailed description of the novel C-band device. Section 3 outlines the basic theory analysis of the novel device. Section 4 discusses the simulation results of the proposed device. Finally, Section 5 presents some conclusions drawn from the present study.

2. Model of description

The mentioned device model with cylindrical symmetry along the Z axis is shown in Fig. 1. This figure shows that the transit-time oscillator mainly contains the following sections: an annular cathode, two opening foils for improving the stability of IREB, a dual-cavity buncher, a single-cavity extractor, and a coaxial output structure to output microwaves. The proposed TTO has the advantages of a simple structure, short axial length, high power efficiency, and low external guiding magnetic field. The operation of the device can be described as follows: when the device starts to work, the annular electron beam propagates axially under the guidance of the external magnetic field. Then, mirror-image charges are generated on the foils when the electron beam passes through the opening foils. These charges then exert a radial force on the electron beam, counteracting part of its radial diffusion force. Thus, when the electron beam passes through the opening foil, its stability is improved. Once the electron beam enters into the buncher, the microwave is excited and it reacts on the electron beam, thereby modulating the velocity of the electron beam. After drifting a distance , the electron beam changes from velocity modulation to density modulation. Finally, the clustered electron beam interacts with the electric field in the extractor and radiates HPM through the coaxial output structure.

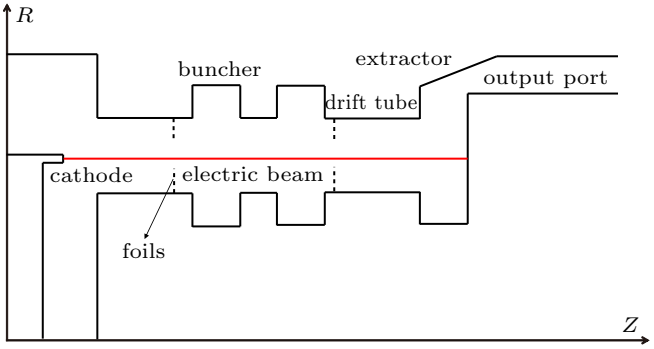


Fig. 1. Model structure.

3. Basic theoretical analysis

This section introduces the main features and working mechanism of the proposed device.

3.1. Electron beam transmission characteristics under the condition of low magnetic field

The introduction of the opening foil is the significant feature of the proposed device. Generally, due to the space charge field, the electron beam propagating in the vacuum tends to diverge.

For some traditional HPM generation devices without external magnetic field, the conductive foils are generally loaded in the beam–wave interaction area to keep the electron beam from diverging. Since the mirror charge generated in the foils can reduce the self-electric field of electrons, the electron beam can be stably transmitted under the action of the self-magnetic field alone. In order to avoid generating the plasma when the electron beam bombards the conducting foil, and to make use of the focusing force of the foil, we hollow out the foil and apply a small amount of external magnetic field. We establish the model shown in Fig. 2 to analyze the focusing force generated by the foil.

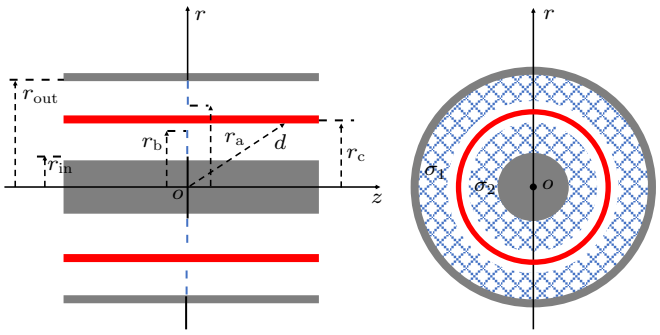


Fig. 2. Opening foil-focused beam in coaxial waveguide.

The equation of electron motion is derived as

$$\frac{\partial \boldsymbol{p}}{\partial t} = \boldsymbol{F}. \tag{1}$$

The component formula in the radial direction is

$$\frac{\partial}{\partial t}\left(\gamma m\frac{\partial r}{\partial t}\right)=-e(E_{\rm r}-v_zB_\theta), \tag{2}$$

where $E_{\rm r}$ and B_θ are the electric field and magnetic field generated by the electron beam in the radial direction and angular direction, respectively. The radial velocity and angular velocity of the electron beam are ignored, and only the axial velocity v_z is considered.

When the foil is loaded, equation (2) can be expressed as

$$\frac{\partial}{\partial t}\left(\gamma m\frac{\partial r}{\partial t}\right)=-e(E_{\rm r1}-E_{\rm r2}-v_zB_\theta), \tag{3}$$

where $E_{\rm r1}$ is the radial electric field generated by the electrons, and $E_{\rm r2}$ is the radial electric field due to the foil.

We established the model shown in Fig. 3 to analyze the radial electric field $E_{\rm r2}$ generated by the foil. Supposing that the charge density of the foil is σ, the observation point P is in the Z–Y plane, and the foil with radius R_0 is in the X–Y plane.

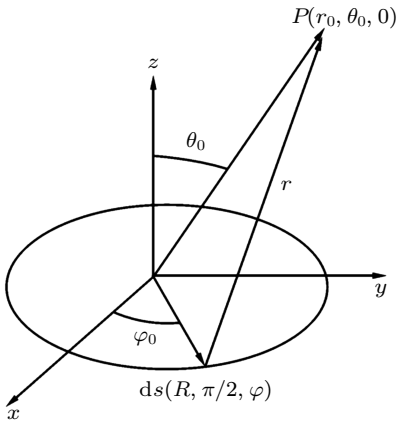


Fig. 3. Schematic diagram of foils in coordinate system.

According to the point charge field strength formula, the radial electric field at point P can be expressed as

$$\iint\frac{\sigma R\,{\rm d}R\,{\rm d}\varphi(r_0\sin\theta_0-R\sin\varphi)}{4\pi\varepsilon_0 r^3}. \tag{4}$$

From the axisymmetric property, it can be known that E_y is the radial electric field intensity generated by the foil at each point in space. $1/r^3$ in formula (4) can be expanded using Taylor series as follows:

$$\frac{1}{r^3}\approx\frac{1}{R'^3}\left(1+\frac{3t}{2}+\frac{15t^2}{2^2}+\frac{3\cdot5\cdot7t^3}{2^3}+\cdots\right), \tag{5}$$

where $R'=(R^2+r_0^2)^{1/2}$ and $t=2Rr_0\sin\theta_0\sin\varphi/R'^2$. By substituting Eq. (5) into Eq. (4) and utilizing the first two terms of the series, E_y can be expressed as

$$E_y=\frac{\sigma\sin\theta_0}{2\varepsilon_0}\left[\frac{3r_0R_0^2+2r_0^3}{2(r_0^2+R_0^2)^{3/2}}-\frac{r_0}{(r_0^2+R_0^2)^{1/2}}\right]. \tag{6}$$

From Eq. (6), the radial electric field generated by the opening foil on the beam envelope at the distance d from the origin can thus be expressed as

$$\begin{aligned}E_{\rm r2}=&\frac{\sigma_1 r_{\rm c}}{2\varepsilon_0 d}\left[\frac{3dr_{\rm out}^2+2d^3}{2(d^2+r_{\rm out}^2)^{3/2}}-\frac{d}{(d^2+r_{\rm out}^2)^{1/2}}\right]\\&-\frac{\sigma_1 r_{\rm c}}{2\varepsilon_0 d}\left[\frac{3dr_{\rm a}^2+2d^3}{2(d^2+r_{\rm a}^2)^{3/2}}-\frac{d}{(d^2+r_{\rm a}^2)^{1/2}}\right]\\&+\frac{\sigma_2 r_{\rm c}}{2\varepsilon_0 d}\left[\frac{3dr_{\rm b}^2+2d^3}{2(d^2+r_{\rm b}^2)^{3/2}}-\frac{d}{(d^2+r_{\rm b}^2)^{1/2}}\right]\\&-\frac{\sigma_2 r_{\rm c}}{2\varepsilon_0 d}\left[\frac{3dr_{\rm in}^2+2d^3}{2(d^2+r_{\rm in}^2)^{3/2}}-\frac{d}{(d^2+r_{\rm in}^2)^{1/2}}\right].\end{aligned} \tag{7}$$

From Eq. (7), we can qualitatively analyze the effect of distance d and the opening size on the radial electric field. A larger distance d and opening size result in a smaller radial electric field. The variation of $E_{\rm r2}$ with opening size is shown in Fig. 4.

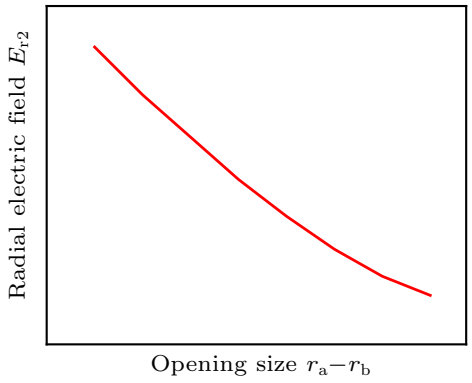


Fig. 4. Plot of electric field $E_{\rm r2}$ *versus* opening size.

To further explain the functions of the opening foil, a 660-kV, 13.6-kA annular IREB is introduced into the transit-time oscillator buncher loaded with two opening foils, and the external guiding magnetic field is 0.4 T. The mentioned transit-time oscillator buncher is shown in Fig. 5, and it is composed of three main parts: a widely-used axial cathode, two opening foils for counterbalancing the space charge force of the IREB, and a dual-cavity buncher. From the figure, it can be seen that when the device is operated, the electron beam does not bombard the foils, thus no pulse shortening occurs. This means the device can operate stably under the condition of low magnetic field.

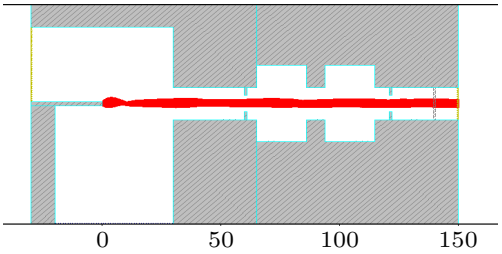


Fig. 5. TTO buncher with two opening foils.

3.2. Pattern analysis

As the IREB travels through the proposed dual-cavity TTO buncher, a series of transverse magnetic (TM) modes is excited. Each TM mode contains 0 and quasi-π modes. The diode voltage range can help determine which mode can interact with the IREB according to the small signal theory. The relative electron conductance ratios of the different modes are illustrated in Fig. 6. Based on the voltage available in the laboratory, it can be known from the electronic conductance that only the mode of TM_{01} mode can be generated when the diode voltage ranges from 197 kV to 2.5 MV.

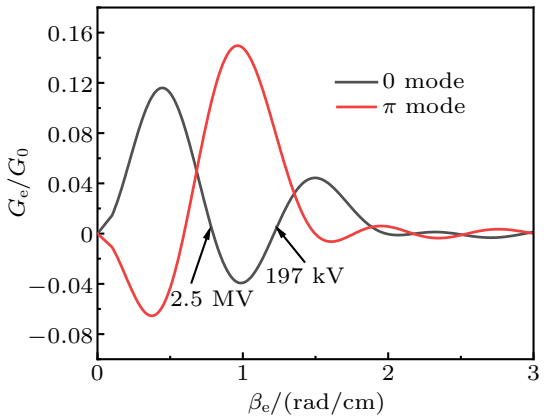


Fig. 6. Plots of electron conductance G_e/G_0 *versus* phase constant for different modes.

Figure 7 shows the electric field of the 0 mode of TM_{01} mode in the buncher. The IREB can be completely modulated when the emission position of the electron beam is set to be at the strongest field strength. Furthermore, positioning the loaded electron beam away from the device surface reduces the risk of the electron beam hitting the device.

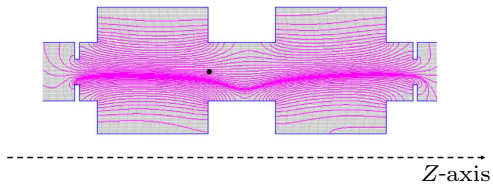


Fig. 7. Field distribution associated with 0 mode of TM_{01} mode.

3.3. Beam–wave interaction analysis

For higher cavity quality factor, the starting current tends to decrease which means that the device is easier to start the oscillations.[11] In order to verify this characteristic, we detect the cavity quality factor of buncher before and after loading the foil as shown in Fig. 8. It can be seen from the figure that the cavity quality factor of the buncher significantly increases when the foil is loaded.

Figure 9 illustrates the changes of electric field within the buncher with time. It is obvious that the saturation time is shortened by about 20 ns after the opening foils loaded.

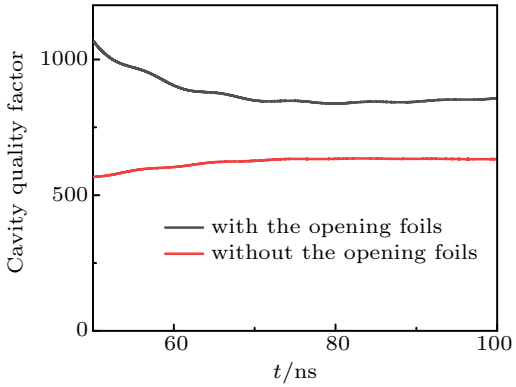


Fig. 8. Cavity quality factor of buncher.

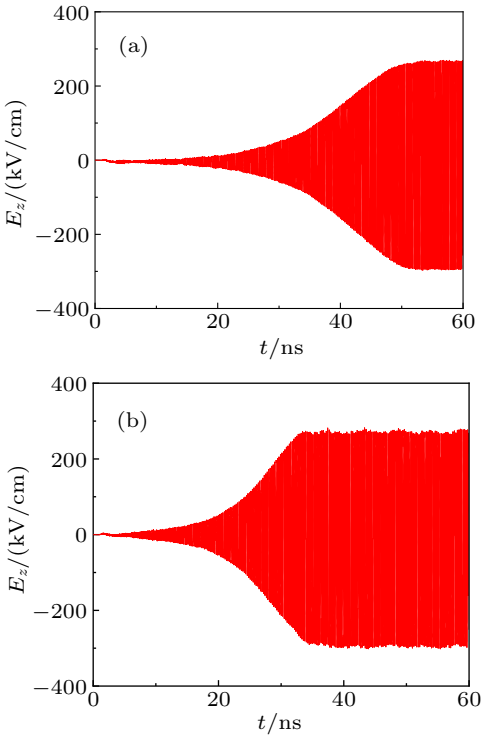


Fig. 9. Electric field E_z *versus* time in the cases (a) without and (b) with opening foil.

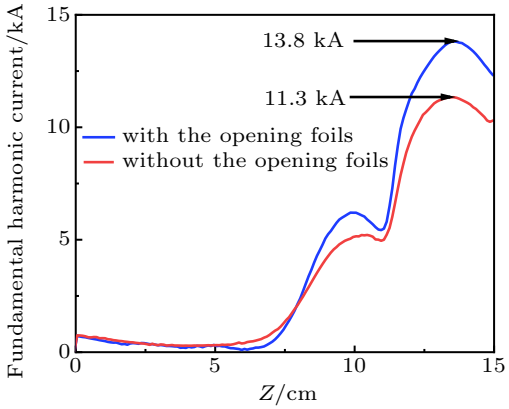


Fig. 10. Fundamental harmonic current along axial direction.

The fundamental harmonic current of the buncher, which illustrates the bunching effect, is presented in Fig. 10. It can be observed from the figure that the fundamental harmonic current increases by 22% after the opening foils have been loaded,

which implies that the beam–wave interaction is more complete due to the improved transmission stability of the IREB.

According to the previous analysis, the smaller the opening size $(r_a - r_b)$, the higher the stability of the electron beam is. The fundamental currents with different opening sizes are shown in Fig. 11.

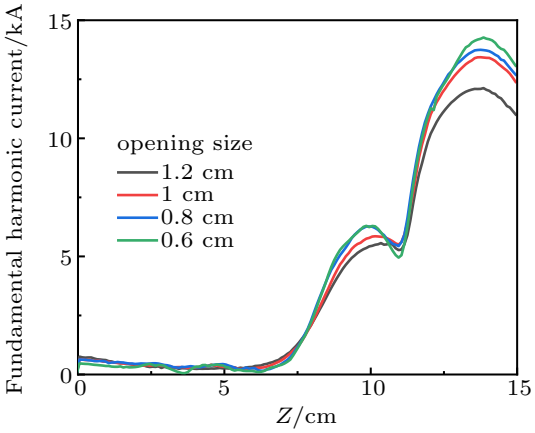


Fig. 11. Fundamental currents with different opening sizes.

According to the results of the above calculations and simulations we add an opening foil to the TTO and conduct the simulation tests.

4. Simulation results

As can be seen in the schematic diagram of the proposed TTO presented in Fig. 1, this TTO has a dual-cavity buncher, a single-cavity extractor and two opening foils. Although the external guiding magnetic field is only 0.4 T, the focusing effect of the opening foils on IREB causes the beam–wave interaction intensity in the buncher to be relatively high level. After the electron beam enters into the extractor through the drift tube, electrons interact with the electric field in the extractor and lose energy to the microwave. Finally, microwave radiates out through the coaxial waveguide.

The results of PIC simulation under 548-kV cathode voltage, 11.4-kA current input, and 0.4-T external magnetic field are shown below.

As shown in Fig. 12, the fundamental current peaks at 14.7 kA before the electron beam reaches extractor, which means that the electron beam has a better clustering effect after passing through the buncher and drift tube. When the IREB enters into the extractor, the beam–wave interaction makes the fundamental current decrease significantly.

Figure 13 indicates the change of electric field E_z within the extractor with time and the spectrum of the output microwave. The amplitude of E_z increases gradually with time and reaches saturation at 24 ns, and its maximum amplitude is 250 kV/cm. Such a strong field would allow more energy to be extracted from the electron beam. The frequency spectrum shows that the output microwave frequency is 4.27 GHz.

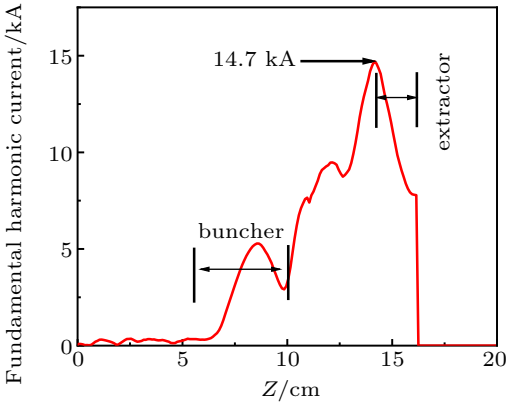


Fig. 12. Fundamental harmonic current along axial direction.

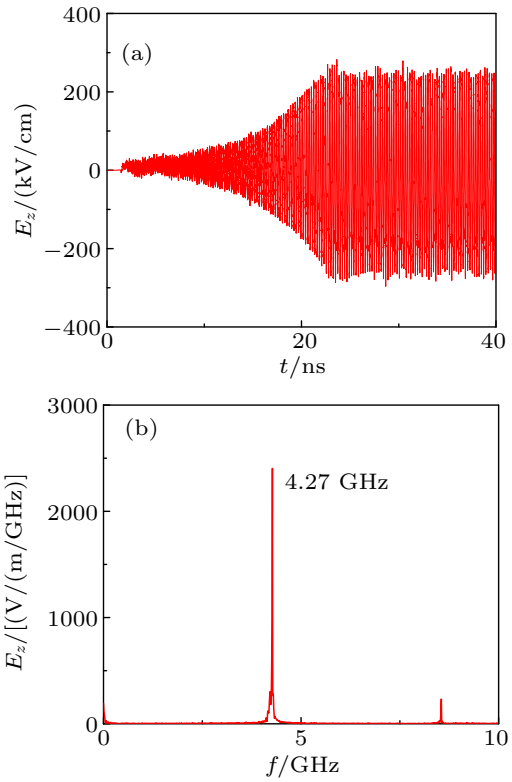


Fig. 13. (a) Plot of electric field E_z *versus* time and (b) frequency spectrum of output microwave.

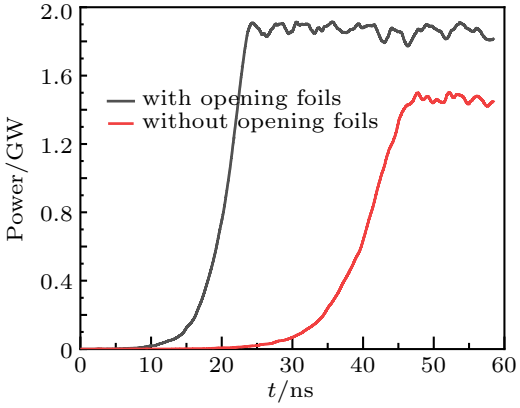


Fig. 14. Curves of output power *versus* time.

Figure 14 shows the variation of the output microwave power with time. Here, the results show the comparison between output power with opening foils and that without opening foils. The average output microwave power values for the two conditions are about 1.88 GW and 1.42 GW, respectively. The power conversion efficiency of the device is 30% with opening foils and 21% without opening foils, indicating a difference of 9%. The corresponding saturation times are 24 ns and 48 ns, respectively, which indicates that the foils can help accelerate device saturation.

5. Conclusions

In this paper, we proposed a novel compact and lightweight coaxial C-band TTO with a 0.4-T external guiding magnetic field. A conductive foil is added to the device for improving the stability of the IREB under the condition of low magnetic field. The quality factor of the device is also enhanced by the introduction of the conducting foil, as it significantly shortens the saturation time of the device. The opening design of the conductive foil gives the proposed device the capability to operate at long pulses and high repetition rates in future experiments. In our simulation, it is observed that when 548-kV diode voltage and 11.4-kA current are input into the device, at a frequency of 4.27 GHz, the average microwave output power is about 1.88 GW, which means that the power conversion efficiency is 30%.

References

[1] Klimov A I, Korovin S D, Rostov V V and Tot'meninov E M 2006 *Phys. Lett.* **32** 120

[2] Totmeninov E M, Klimov A I and Rostov V V 2010 *IEEE Trans. Plasma Sci.* **38** 2944

[3] Totmeninov E M, Kitsanov S A and Vykhodtsev P V 2011 *IEEE Trans. Plasma Sci.* **39** 1150

[4] Tot'meninov E M, Stepchenko A S, Rostov V V and Klimov A I 2018 *Technical Phys.* **63** 581

[5] Haworth M D, Baca G, Benford J, Englert T, Hackett K, Hendricks K J, Henley D, LaCour M, Lemke R W, Price D, Ralph D, Sena M, Shiffler D and Spencer T A 1998 *IEEE Trans. Plasma Sci.* **26** 312

[6] Fan Y W, Shu T, Liu Y G, Huang H Z, Li Z Q, Wang Y, Zhao Y S and Luo L 2005 *Chin. Phys. Lett.* **22** 164

[7] Li Z Q, Zhong H H, Fan Y W, Shu T, Qian B L, Xu L R and Zhao Y S 2009 *Chin. Phys. Lett.* **26** 055201

[8] Cao Y B, Zhang J D and He J T 2009 *Phys. Plasmas* **16** 083102

[9] Cao Y B, He J T, Zhang J D, Zhang Q and Ling J P 2012 *Phys. Plasmas* **19** 072106

[10] Ling J P, Zhang J D, He J T and Jiang T 2014 *Phys. Plasmas* **21** 023114

[11] Levush B, Antonsen T M, Bromborsky A, Lou W-R and Carmel Y 1992 *IEEE Trans. Plasma Sci.* **20** 263